Solar Energy Materials and Solar Cells 173 (2017) 33–36

Contents lists available at ScienceDirect

Solar Energy Materials and Solar Cells

journal homepage: www.elsevier.com/locate/solmat

On the equilibrium concentration of boron-oxygen defects in crystalline silicon

D.C. Walter[a,*], R. Falster[b], V.V. Voronkov[b], J. Schmidt[a,c]

[a] Institute for Solar Energy Research Hamelin (ISFH), Am Ohrberg 1, 31860 Emmerthal, Germany
[b] SunEdison Semiconductor, Via Nazionale 59, 39012 Merano, Italy
[c] Department of Solar Energy, Institute of Solid-State Physics, Leibniz Universität Hannover, Appelstr. 2, 30167 Hanover, Germany

ARTICLE INFO

Keywords:
Czochralski silicon
Boron-oxygen defects
Carrier lifetime

ABSTRACT

We determine the equilibrium concentration of the BO defect in boron-doped Czochralski-grown silicon after prolonged (up to 150 h) annealing at relatively low temperatures between 200 and 300 °C. We show that after sample processing, the BO concentration has not necessarily reached the equilibrium state. The actually reached state depends on the detailed temperature profile of the last temperature treatment before the light-induced degradation (LID) is performed. For the investigated Cz-Si materials with base resistivities ranging between 0.5 and 2.5 Ω cm, we observe that an annealing step at 200 °C for 50 h establishes the equilibrium, independent of the base resistivity. Experiments performed at different temperatures reveal that the equilibrium defect concentration decreases with increasing annealing temperature. This observation can be understood, assuming a mobile species which is distributed between at least two different sinks. A possible defect model is discussed.

1. Introduction

In boron-doped and oxygen-rich silicon, the carrier lifetime is limited by a recombination centre which is related to a defect complex containing both of these elements, boron and oxygen [1–3]. This BO-related defect complex reveals its recombination-active properties under illumination at room temperature, leading to a degrading lifetime upon illumination over several hours, if started from a recombination-inactive defect state. This effect is often referred to as light-induced degradation (LID), although the excess electron concentration is actually causing the degradation rather than photons [4]. The recombination-inactive state, corresponding to a high carrier lifetime, can be reached by annealing the samples in darkness, e.g. at 200 °C for 10 min. However, this high lifetime – in the following denoted τ_0 – is not stable upon renewed illumination but degrades again towards the degraded lifetime value τ_d. As it was shown previously, the switching between these two states is completely reversible [2].

Within this paper, we show that the lifetime τ_d and, hence, also the effective defect concentration N_d^*, may change upon annealing the samples at relatively low temperatures between 200 and 300 °C, if the responsible defect complex has not reached an equilibrium. Interestingly, the time span needed to reach this equilibrium, which we determine in this study to be around 50 h, is independent of the doping concentration of the silicon sample for doping concentrations between 5.7×10^{15} cm^{-3} and 3.3×10^{16} cm^{-3}. Additionally, we observe that the equilibrium defect concentration $N_{d,eq}^*$ depends on the annealing temperature applied to reach the equilibrium. We explain the results presented here within the framework of a defect model which consists of a mobile species which is distributed between two different sinks. One of these sinks forms together with the mobile species the BO-related defect complex, while the other sink features no or only minor recombination properties.

2. Experimental details

We use boron-doped Cz-Si wafers with different base resistivities ranging between 0.5 and 2.5 Ω cm. The wafers are cut into samples of either 2.5 × 2.5 cm^2 or 5.0 × 5.0 cm^2 in size. Sample processing includes the removal of the surface damage using an aqueous solution of KOH. After sample cleaning in a standard RCA cleaning sequence, all samples undergo a phosphorus diffusion (847 °C for 51 min), which results in n^+-regions with a sheet resistance of 100 Ω/□ on both wafer surfaces. Subsequently, the phosphosilicate glass (PSG) and the n^+-regions are removed using HF and KOH, respectively. After another RCA cleaning, the surfaces of the samples are passivated by the deposition of 10 nm Al_2O_3 via plasma-assisted atomic layer deposition. Finally, the samples are annealed at 425 °C for 15 min in ambient environment to activate the Al_2O_3 surface passivation [5].

* Corresponding author.
E-mail address: d.walter@isfh.de (D.C. Walter).

http://dx.doi.org/10.1016/j.solmat.2017.06.036
Received 31 March 2017; Received in revised form 16 June 2017; Accepted 19 June 2017
Available online 03 July 2017

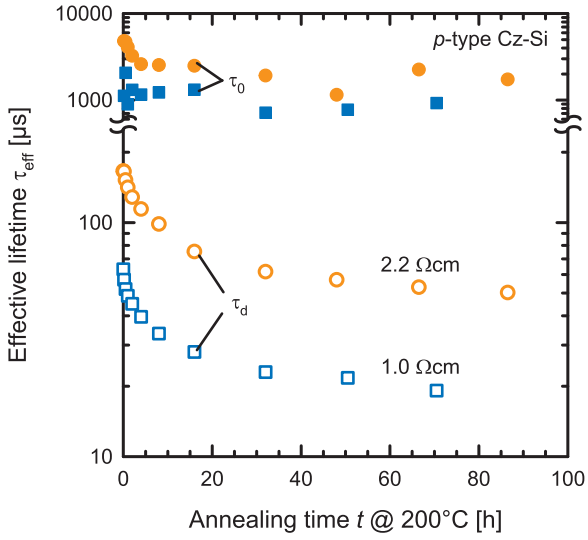

Fig. 1. Measured effective lifetimes τ_{eff} of two samples with a resistivity of 2.2 Ω cm (orange circles) and 1.0 Ω cm (blue squares) plotted versus the annealing time t at 200 °C. The lifetimes after annealing in darkness τ_0 (full symbols) and after complete LID τ_d (open symbols) are shown. Over the course of 80 h annealing τ_d shows an exponential degradation. (For interpretation of the references to color in this figure legend, the reader is referred to the web version of this article.)

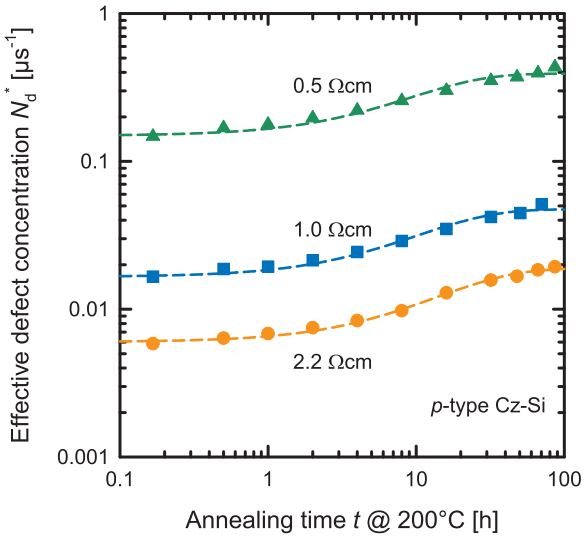

Fig. 2. Effective defect concentration N_d^* of three lifetime samples with different base resistivities (triangles: 0.5 Ω cm, squares 1.0 Ω cm and circles: 2.2 Ω cm) plotted versus the annealing time t at 200 °C. Please note, the values of the 0.5 Ω cm sample are extracted at $\Delta n = 0.5\times10^{14}$ cm^{-3} otherwise an injection level of $\Delta n/p_0 = 0.1$ is chosen. The dashed lines are mono-exponential fits of the data points.

Lifetime measurements are performed using the lifetime tester WCT-120 from Sinton Instruments. If not stated otherwise, all lifetimes in the following are extracted at $\Delta n = 0.1\times p_0$, with the excess carrier density Δn and the hole concentration in darkness p_0.

3. Results and discussion

3.1. Adjusting the equilibrium

In Fig. 1, the change of the lifetimes τ_0 and τ_d upon annealing at 200 °C is shown for two different samples with 1.0 and 2.2 Ω cm base resistivity. After each annealing step, the lifetime τ_0 is measured. Afterwards, the lifetime samples are illuminated at 40 °C for 20 h, using a halogen lamp with an illumination intensity of $P_{ill} = 10$ mW/cm^2, to reach the fully degraded state. Then, the lifetime τ_d is measured. As can be seen from Fig. 1, the lifetime after annealing remains almost stable on a very high level, higher than 700 µs for the 1.0 Ω cm material and higher than 1.9 ms for the 2.2 Ω cm. Hence, we conclude that the surface passivation quality remains on a high and stable level during the course of the experiment. This interpretation is further supported by float-zone (FZ-Si) wafers processed in parallel. On the 1.3 Ω cm FZ-Si wafers we measure a slight degradation from 2.6 to 1.6 ms over the course of 80 h annealing at 200 °C. The lifetime after complete LID, τ_d, however, shows an exponential decay until a saturation value $\tau_{d.eq}$ is reached.

From the measured lifetimes τ_d and τ_0 we calculate the effective defect concentration using the equation $N_d^* = \tau_d^{-1} - \tau_0^{-1}$. Fig. 2 shows the evolution of the effective defect concentration upon annealing at 200 °C. For all examined materials, we observe an exponential increase of the defect concentration until a saturation value $N_{d.eq}^*$ is reached. The dashed lines in Fig. 2 are mono-exponential fits of the form $N_d^* = y_0 + a\times(1-\exp(-\gamma \times t))$, with γ being the equilibration rate constant. We find a rate constant of $\gamma(200°C) = (0.06 \pm 0.01)\,h^{-1}$ independent of the base doping concentration.

On another set of lifetime samples, we examine the defect concentration on an even longer time scale by annealing the samples subsequently three times for 50 h at 200 °C and determine N_d^* after 50 h, 100 h and 150 h. Fig. 3 shows N_d^* plotted versus the annealing time at 200 °C for three different samples with base resistivities ranging between 0.5 and 2.5 Ω cm. In-between the lifetime measurements of τ_0 and τ_d after each annealing step, the samples are illuminated at room temperature longer than 100 h using a halogen lamp with an illumination intensity of $P_{ill} = 10$ mW/cm^2. For annealing times longer than 50 h no change of N_d^* can be observed for these samples. This suggests that the equilibrium state – characterized by the equilibrium defect concentration $N_{d.eq}^*$ – is reached within 50 h of annealing time for all samples, independent of the base resistivity.

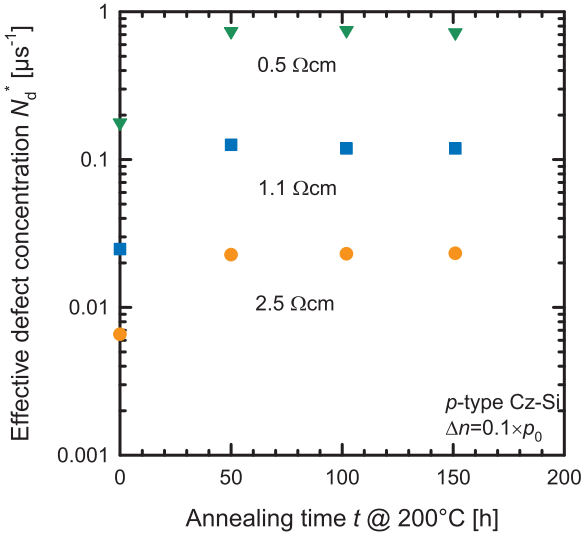

Fig. 3. Effective defect concentration N_d^* plotted versus annealing time t at 200 °C in darkness for three different samples with different base resistivities. The equilibration process proceeds within the first 50 h of annealing. Longer annealing has no further effect on N_d^*, hence the equilibrium defect concentration $N_{d.eq}^*$ is reached after 50 h of annealing.

3.2. Temperature-dependent defect equilibrium

In addition, we examine the temperature dependence of the equilibrium defect concentration $N_{d.eq}^*$ by annealing the same samples in darkness for 50 h at different temperatures in the following sequence: 240 °C, 220 °C, 200 °C and 300 °C. At the end of this sequence, we add additionally a short annealing step at 425 °C for 15 min. We added this short annealing step to compare the defect concentration measured